DYNAMICS OF ENSO EVENTS IN THE INDIAN OCEAN : TO WHAT EXTENT WOULD RECRUITMENT AND CATCHABILITY OF TROPICAL TUNAS BE AFFECTED ?

Marsac, F [1] and Jean-Luc Le Blanc[2]

ABSTRACT

*In this paper, the authors explore functional relationships between environmental fluctuations and some key parameters used in stock assessment such as recruitment and catchability. Yellowfin tuna (*Thunnus albacares*) is taken as an example but the concepts developed in this study could be widened to other tropical tunas. The French purse seine data-set is used to estimate a recruitment index from adjusted CPUE of age 0 fishes, and the effect of the environment on catchability is assessed using CPUE of age 3 fishes which provide the bulk of adult catches. The ACE algorithm is used to describe a non-linear relationship between the recruitment and the turbulence (wind speed cubed). There is a detrimental effect of an increasing turbulence on recruitment. The optimal transformation of this simple regression explains more than 25 % of the variance of recruitment. The analogy, with the fundamental triad and the optimal environmental window that explain the variability of small pelagic fish populations, is discussed. Regarding catchability, there is clearly a non-linear relationship between the CPUE age 3 and the depth of the isotherm 20°C (denoting the core of the thermocline), with a negative effect of deeper thermocline. These results are used to assess the potential effects of the El Niño-Southern Oscillation (ENSO) events on tuna stocks and their exploitation. The dynamics of ENSO in the Indian Ocean are described, and it appears that the latest event (1997-98) will remain classified in this ocean as extremely intense. The fishing pattern of purse seiners changed drastically: an abnormal easterly wind stress along the equator induced a reversal of the slope of the ocean (and consequently that of the thermocline). Rising of thermocline in the eastern basin generated increased catchability for purse seine gears. It is also suggested that ENSO would promote success of recruitment for tropical tunas. However, the consequence for the stock is not straightforward, as the response might be related to its level of exploitation.*

RESUME

*Dans cet article, les auteurs examinent des relations fonctionnelles entre les fluctuations environnementales et des facteurs clés de l'évaluation de stocks comme le recrutement et la capturabilité. L'albacore (*Thunnus albacares*) est pris comme exemple mais les concepts développés dans cette étude pourraient être élargis à d'autres thons tropicaux. Les données françaises de pêche à la senne sont utilisées pour estimer un indice de recrutement à partir des CPUE des individus d'âge 0, et l'effet de l'environnement sur la capturabilité est évalué au travers de la CPUE des individus d'âge 3 qui dominent les prises d'adultes. L'algorithme ACE est utilisé pour décrire une relation non linéaire entre le recrutement et la turbulence (vitesse du vent au cube). L'effet néfaste d'une turbulence élevée sur le recrutement est mise en évidence. La transformation optimale de cette régression simple explique plus de 25 % de la variance du recrutement. L'analogie avec la triade fondamentale et la fenêtre environnementale optimale qui permet d'expliquer la variabilité des populations de petits pélagiques, est discutée. S'agissant de la capturabilité, il apparaît clairement une relation non linéaire entre la CPUE d'âge 3 et la profondeur de l'isotherme 20°C (signalant le cœur de la thermocline), avec un effet négatif d'une thermocline profonde. Ces résultats sont utilisés pour évaluer les effets potentiels des phénomènes El Nino-Oscillation Australe (ENSO) sur les stocks de thons et leur exploitation. La dynamique des ENSO dans l'océan Indien est décrite : il apparaît que le dernier en date (1997-98) restera comme un événement d'intensité exceptionnelle dans cet océan. L'activité de pêche à la senne a été profondément modifiée : une tension de vent anormalement forte vers l'ouest à l'équateur a entraîné une inversion de la pente de la surface de l'océan (et par conséquent de la thermocline). L'élévation de la thermocline dans le bassin est a induit une capturabilité accrue à la senne. Il est également suggéré que l'ENSO favoriserait le succès du recrutement des thons tropicaux. Cependant, les conséquences effectives sur le stock ne peuvent être déduites directement car la réponse est vraisemblablement variable selon son niveau d'exploitation.*

Introduction

Increasing interest has been focused on ENSO events during the last decades because of their climatic, ecological and economic consequences. This has long been a topic studied mostly by climatologists and oceanographers in order to understand the mechanisms of the phenomenon. The biological effects were first considered in the Eastern Pacific Ocean (Galapagos, Peru and Ecuador) where the environmental anomalies were highly developed, with subsequent collapse of seabird populations and pelagic fisheries. The consequences on tuna populations were assessed in the purse seine fishery monitored by the IATTC (see IATTC annual reports since 1983) and in the Japanese longline fishery (Suzuki, 1988). These studies point out the effect on catchability, with a detrimental effect of the El Niño events on purse seining in the Eastern Pacific yellowfin tuna fishery and positive effects for longlines. The effects on abundance were also assessed and it appeared that strong year classes were generated during El Niño years.

In general, such studies require long series of data. The ENSO cycle ranges between 4 and 6 years and the fishery data to be considered need to cover at least 10 to 12 years in order to implement consistent analyses. In the Indian Ocean,

[1] IRD (Institut de Recherche pour le Développement), HEA, BP 5045, 34032 Montpellier Cedex, France.
[2] Southampton Oceanographic Centre, Department of Oceanography, UK.

the purse seine fishery started on a commercial basis in 1984, and we have now compiled a series of observations compatible with this type of analysis. The environment is known to play a role on the dynamics of tuna fisheries, but the underlying processes controlling recruitment and catchability are not much emphasized. On the other hand, bio-ecological concepts explaining the success of recruitment were hypothesized on small pelagic fisheries (Lasker 1981; Parrish *et al* 1981; Cury and Roy 1989; Bakun 1995) and a number of papers have rather confirmed their validity. The purpose of the present paper is to test these ideas on tunas, taking yellowfin as an example, in order to estimate the potential consequences of the Indian Ocean ENSOs on the tropical tuna stocks and their exploitation.

Data and methods

Physical data

Sea level pressure (SLP)

The SLP is a major parameter driving the atmospheric circulation. In the Pacific, the changes of the Southern Oscillation are depicted by an index which is the difference between standardized SLP anomalies in two distant locations, Darwin (12°30'S, 131°E), Australia, and Tahiti (French Polynesia). This index is a good indicator of the dynamics of the ENSO events. We computed a similar index specific to the Indian Ocean, namely the Indian Ocean Index (IOI), from the SLP anomalies measured in Seychelles (Mahé airport, 4°S-55°E) and Darwin. The data from Darwin are easily available on the Web. Those of Mahé were kindly provided by the Seychelles Meteorological Office which has been recording the SLP on a daily basis since 1972. The IOI is the difference between the monthly standardized anomalies at the reference locations ("Seychelles" minus "Darwin").

Surface parameters

In this paper, three major surface parameters are used, SST, scalar wind and the east-west component of the pseudo wind stress. The wind stress is the product of the air density, the drag coefficient, the wind vector and the scalar wind (i.e. wind speed). The pseudo wind stress is limited to the two last terms of this product.

Those parameters are extracted from COADS (see Slutz *et al* 1985, Woodruff *et al* 1987). This data set is the richest source of surface records ever made available. On the global scale, there are more than 100 million measurements made since 1854. The latest release covers the period 1950-1995. The data are extracted using a specific program (CODE: Mendelssohn and Roy 1996) that computes statistics at different spatial (0.5°x0.5°, 1°x1°, 2°x2°, or the whole area selected) and temporal levels (day, month, year).

Another source of pseudo wind stress, provided by the Florida State University, is also analyzed. The data were computed on a 1°x1° grid monthly, since 1970.

Subsurface parameters

A great number of oceanographic stations (>13,000 in the Western Indian Ocean) and vertical temperature profiles (>61,000) were compiled in a specific database and processed by an oceanographic applications manager (GAO system) developed by ORSTOM (F. Marsac). Most of the data come from the World Ocean Atlas of the NOAA-NESDIS (Levitus and Boyer 1994) and the TOGA and WOCE programs. So far, the database handles data for 1906-1995, but an update for recent years is under process.

For the purpose of this paper, we have computed the depth of the 20°C isotherm, which is considered to track the core of the thermocline.

Catch and effort data

Two specific aspects of population dynamics, abundance and catchability, are addressed in this paper. Abundance can be studied from recruitment indices provided by different means (GLM, cohort analysis, CPUE). Due to the lack of recent catch and effort data for all gears, we only focused on CPUE analysis of the French purse seine data set for 1984-96. We also considered yellowfin tuna alone, as this is one of the main species exploited by purse seines.

The fishing effort provided by the purse seiner logbooks has to be standardized and adjusted to reflect the heterogeneity of the fleet and the increasing efficiency of the vessels. Standardization takes into account the various individual fishing powers of the vessels to provide a comparable fishing effort at the level of the fleet.

CPUEs computed from the standardized effort exhibit an increasing trend. It is very likely that this reflects a greater efficiency of the vessels and not an increase of abundance. An increase in efficiency would be a logical consequence of several factors, such as the fishers learning about the area, improvement of the fishing gear (deeper nets and faster windlasses) and the progressive deployment of very sophisticated electronic equipment (sonar, bird radar, radio beacons on floating objects…). Therefore, an annual efficiency rate for the whole fleet has to be estimated to adjust the trend of CPUEs. There are few references regarding this point. We have used the approximation to an annual rate of 3 % proposed by Gascuel *et al.* (1993) for the purse seiners fleets operating in the Atlantic Ocean, and this value was used to calculate an adjusted effort.

The catch-at-age for yellowfin is estimated using the extrapolated length frequency distributions and a slicing table (Marsac 1992) that gives size limits for each month at each age. The corresponding adjusted CPUEs at age are obtained by dividing the catch-at-age by the adjusted effort expressed in search time (i.e. fishing time from which the time spent setting is removed).

Methods

Empirical Orthogonal Functions (EOF)

A method using EOFs, a technique derived from the principal component analysis, has been extensively used in meteorology and oceanography to analyze space and time trends in data sets (Lorenz 1956). The method represents the data as a sum of products of functions: $f(x,y,t) = \Sigma (Fi(x,y) . Gi(x,y)$ where F*i* denotes the data distribution in space and G*i* gives the contribution of the respective space distribution at any given time. An infinite sum of functions will reproduce the current observations but, practically, the summation is truncated after the first few terms. The contributions of the sum are arranged in such a way that the first term (= first axis) accounts for more of the variance

found in the observations than any other term. The second term accounts for most of the remaining variance and so on. The Eigen values that are calculated by this method have no unit and are proportional to deviations about the mean (standardized anomalies). The product of the spatial value (or coefficient) for the grid point (x,y) and the value at time t gives the sign of the anomaly for the triplet (x,y,t).

Non-linear statistics

The functional relationships between the environment and the resource are carried out using non-linear methods. These techniques have become rather common in ecology and particularly two of them, GAM (Generalized Additive Modelling) and ACE (Alternating Conditional Expectation). The latter is used in the present study. This iterative algorithm (Breiman and Friedman 1985) estimates empirically optimal transformations for simple or multiple regressions. The response variable Y and the independent variables X_1, …., X_n are replaced with functions $T_1(Y)$ and $T_2(X_1)$, …., $T_{n+1}(X_n)$ that are estimated using minimizing procedures (see Cury and Roy 1989 for more details).

Characteristics of the fishery

The current fishing grounds of the purse seine fishery are given in Figure 1. This fishery is characterized by two distinct activities: setting on schools associated to floating objects, and setting on free swimming schools. The drifting objects, either natural or artificial (specially designed rafts) which provide a greater success rate for the sets, are now extensively used (60 to 75 % of total catch). The geographic distribution of these two types of fishing are mainly related to the surface current pattern. The objects tend to concentrate in the gyres (Somalia during the 3rd quarter, Northern Mozambique Channel) and, to a lesser extent, in the Equatorial Counter Current (ECC), a seasonal zonal current (November to March) flowing eastwards. Skipjack, mixed with small sized yellowfin and bigeye (less than 10 kg) are dominant (in numbers) on objects (Figure 2a). On free schools, the bulk of the catch is made of large yellowfin (FL>100 cm, mode at 140 cm, 55 kg) (Figure 2b).

The three main fishing grounds exhibit a well marked seasonal pattern (Figure 3). The Somali basin is exploited from mid-July to mid-November. The seiners fish mainly on floating objects and skipjack is the dominant species. The Mozambique Channel is another area with significant catches on objects and a corresponding dominance of skipjack. On the other hand, the central area (ECC) is dominated by yellowfin caught on free swimming schools. However, one can still notice in this area a more or less continuous activity on objects throughout the year.

Delimitation of the study area

Considering yellowfin tuna as the main species of interest for the present study, and given the geographical pattern depicted in the previous section, it is clear that the ECC (as shown in Figure 3) can be considered as the appropriate study area to estimate abundance indices.

Refinements regarding the environmental conditions can be obtained through the analysis of the oceanographic features of this area. Indeed, averaging physical values on a wide area without considering the spatial heterogeneity may lead to spurious results about the trend of the climatic conditions.

Therefore, using COADS for 1970-95, we analyzed the trend of SST and scalar wind in 5° longitude boxes, from 45°E to 75°E, all over the ECC area stretching from 2°S to 10°S. The plots are presented in Figure 4. The general shape of the SST increases from the West to the East, and the interannual variability is stronger West of 60°E. Cold years, such as 1975, 1985 and the period 1993-95 in some areas, appear clearly. The 3 western boxes also exhibit a roughly inverse relationship between SST and wind speed. In the eastern boxes (60°E to 75°E), the interannual variability is not as marked as in the west, and both SST and wind speed show a trend increasing slightly with time. An analysis of variance made on these parameters results in significant contributions of both time and space in the trend depicted in the plots. However, a good coherence in the behavior of SST and wind speed is obtained when the 3 eastern boxes are merged together.

Additional information is given by the FSU data set. We computed a turbulence index as the cube of the scalar wind, for the whole Indian Ocean, by 1°x1° and month. An EOF analysis was then carried out on this parameter. More than 75 % of the variance is explained along the 2 first axes of the analysis (Figure 5). The time components of the two axes show an increasing trend, with a sharp transition from a relatively low turbulence in the 1970s to enhanced turbulence conditions starting in the 1980s. The spatial pattern of the first EOF (67 % of variance) points to the weaker turbulence of the equatorial area. It appears that the calmest areas stretch out east of 60°E, which is in accordance with the spatial homogeneity suggested in the previous paragraph for the area 60°E-75°E.

Exploring functional relationships between yellowfin abundance and the environment

The abundance and catchability of yellowfin are estimated in the ECC area. The parameters depicting the surface conditions (SST and turbulence) are computed in the ECC for the area 60°E-75°E, according to the relative homogeneity found in this area. The depth of the 20°C isotherm (Z20) is computed in a more restricted area which encompasses the highest catch rates of the ECC, i.e. 2°S-7°S / 55°E-70°E. The surface parameters are used to explain the changes in cohort abundance whilst Z20 is tested as a factor explaining catchability changes.

Abundance

Abundance is estimated by a recruitment index based on the adjusted CPUE of age 0 yellowfin (namely CPUE 0). For this specific case, CPUE is calculated by combining all types of sets (objects and free schools) because juveniles, that are aggregated around objects, can also mix in free schools with other age groups (Figure 2b). The seasonal pattern of CPUE 0 shows higher values in the second half of the year (Figure 6a). These fishes which are just recruited in the purse seine fishery are 6 to 12 months old and were born during the first quarter of the year. Therefore, the recruitment index of a given year is the average CPUE 0 for the period July-December.

Averages of SST and turbulence were calculated for the first quarter. They represent surface conditions met during the spawning and the first larval stages of the individuals that are considered in the recruitment index 6 months later. The turbulence depicts the mixing intensity of the water column in which the larvae are released. This parameter has been extensively used in different studies dealing with pelagic larval ecology (Lasker 1981, Peterman and Bradford 1987, Parrish *et al* 1981, Cury and Roy 1989). SST and turbulence are well correlated in the recent period (r = -0.72 for 1984-95): high (low) turbulence is associated with low (high) SST.

Obviously, tunas have adapted their reproductive strategy to the environmental conditions. The spawning period, appears to be well in phase with high SST (Figure 6b) and low turbulence (Figure 6c). Peak values of the gonado-somatic index occur from December to March, whilst the maximum turbulence is found in July-August, in relation to the southwest monsoon.

Plots of recruitment index (July-December) and turbulence (January-March) are shown in Figure 6d. During the period under study, it is suggested that lower recruitment matches with high turbulence. This relationship was examined using non-linear statistics (ACE algorithm) for a 12-year period (1984-95). The response variable is forced to be linear to facilitate interpretation. The logarithm of the recruitment index was used in the different transformations for simple (models 1 and 2) and multiple (model 3) regression. The results are as follows:

T_1(recruitment) = T_2(SST), R^2 = 21.9 % (1)

T1(recruitment) = T2(Turbulence)R^2 = 25.8 % (2)

T1(recruitment) = T2(Turbulence) + T3(SST), R^2 = 37.1 %(3)

As mentioned earlier, SST and turbulence are well correlated. Therefore, although a higher R^2 was obtained, we did not consider the results from the multiple regression, and we only kept the simple regression that provides the best percentage of variance explained, i.e. turbulence. The graphic output of model 2 is plotted in figure 7.

The optimal transformation suggests that increased turbulence is detrimental to the recruitment of yellowfin. In a recent study made in the Eastern Atlantic, Marsac (1998b) described a bell-shape response curve of recruitment versus turbulence, with optimal conditions reached around 90 m^3/s^3, that is a wind speed of 4.5 m/s. In the ECC area of the Indian Ocean, the highest recruitment is found at 150 m^3/s^3, that is a wind speed of 5.3 m/s, and the response, though non linear, does not exhibit an "optimal window" shape. A possible explanation is that winds are generally stronger in the Indian Ocean than anywhere else (Tomczak and Godfrey 1994); consequently, we would not observe the left part (low turbulence) of the theoretical bell curve.

Catchability

The environmental effect on catchability is assessed on the large concentrations of free swimming schools occurring during the spawning season. Therefore we have excluded the sets made on objects, and the adjusted age 3 CPUE was selected. Age 3 yellowfin (CPUE 3) contributes mostly to the catches of adult fishes. The seasonal pattern (Figure 8a) indicates peak values during the first quarter of the year. The good agreement of this pattern with the gonado-somatic index denotes the fact that those adults congregate in ECC for spawning.

The average depth of the 20°C isotherm was computed in the area of highest catch rates within the ECC. This parameter exhibits a semi-annual cycle: the thermocline is shallower in May-June and in December-January (Figure 8b). In fact, the seasonal pattern of the adult CPUE lags that of Z20 by one month.

The age 3 CPUE trends were compared with Z20 for the first quarter of each year (1984-95). The two series (Figure 8c) appear to be well in phase: CPUEs decline as the thermocline deepens. Again, optimal transformations were calculated for the simple regression using Z20 : T_1(Log CPUE age 3) = T_2(Z20). This simple model can explain 16.4 % of the variance: the shape of the relationship points to a threshold effect (Figure 9a) with a rather stable CPUE for shallow thermocline (depth <60 m), followed by a sharp decline of the CPUE when the thermocline deepens (70 to 80 m). This relationship indicates that the catchability of the free swimming schools is directly affected by the depth of the mixed layer. This is in perfect agreement with direct observations provided by acoustic tagging, where it is shown that yellowfin spends more of its daily activity about the thermocline gradient (Marsac 1998a).

We also investigated the effect of the cohort strength on CPUE 3, considering a lag of 3 years in the regression. Therefore, the series was reduced to 9 points (Log recruitment 1984-92 vs Log CPUE 3 1987-95). The model explains 11.4 % of variance and the empirical transformation suggests a positive effect of successful recruitment on the CPUE 3 (Figure 9b).

Oceanographic effects induced by ENSO events

The remote climatic connection between Pacific and Indian oceans have been investigated since the 1982-83 ENSO (Barnett 1983, 1984a,b, 1991, Meehl 1987). The surface warming occurring along the coast of Peru is not a local anomaly but the result of a cyclic large scale phenomenon induced by SST and SLP differences along the equatorial Pacific. It has also been demonstrated that the ENSO signal in the Indian Ocean explains as much of the interannual variability in this ocean as it does in the Pacific (Tourre and White 1995).

The spatial pattern of the zonal wind stress exhibits drastic changes during ENSO years. We have analyzed the month of January which corresponds to the ENSO peak phase. The climatological field, for this month, is characterized by weak westerlies (positive zonal wind stress) from 10°S to the equator (Figure 10a). The area so delimited is the wind convergence zone (ITCZ). During "normal" years, the response of the ocean to the westerlies is an eastward surface circulation which tends to elevate the sea level and deepen the thermocline along the Indonesian coast. To balance the hydrostatic pressure, the thermocline is shallower in the western equatorial basin. During ENSO situations, the shape of the ITCZ is modified and is slightly displaced to the South, as observed in January 1983 (Figure 10b). The transition to strong easterlies, North of the equator, is very sharp. Consequently, the surface circulation will be intensified westward, resulting in a thinner mixed layer in the East, and a deeper one in the West. The phenomenon was

particularly extreme during the latest (1997-98) ENSO (Figure 10d). In January 1998, the westerlies of the convergence area totally disappeared, generating an abnormally shallow thermocline in the East and a significant downwelling in the West. Warmer SSTs are associated with the downwelling, generating an active convection, resulting in a higher than normal cloud cover and heavy rains. Contrary to ENSO, La Nina type conditions, as observed in 1986 (Figure 10c), are characterized by strong westerlies in the ITCZ, creating a abnormal raising of the thermocline in the West and intense deepening along the Indonesian coast.

A Hovmoller diagram across the equatorial area (5°N-5°S) is used to compare the different ENSOs observed since 1970 (Figure 11). The more significant ones appear through the shaded area (denoting easterlies in January) crossing the whole basin. This was the case in 1973, 1983, 1995 and 1998, the last being the strongest recorded in the Indian Ocean during the period considered. In the equatorial zone, the westerlies prevail during the 3rd quarter, corresponding to the summer monsoon. The strongest intensity was recorded during two periods, 1973-75 and 1984-86, which were also characterized by lower than normal temperatures (cf. Figure 4) and can be considered as cold years.

It is interesting to note that the yellowfin spawning grounds are located within the wind convergence area seen in the wind stress maps (see Figure 10), where the wind, and consequently the turbulence, are the weakest. In the ECC area, the IOI exhibits a drastic decline during ENSO; therefore, it can be used as a surrogate variable related to the Indian Ocean warm events (Figure 12). During ENSOs, the trade winds are intensified (strong negative component) during the southwest monsoon (July-August). In January-February, i.e. during the spawning season, the wind stress (eastward-oriented) variability is not as important as in July-August, but there is a tendency that weaker wind stress, and consequently weaker turbulence, is associated with a low IOI. According to the relationships described in the previous section, the recruitment of yellowfin would benefit from Indian Ocean warm events, induced by ENSO and tracked by the IOI. On the other hand, the same warm events would decrease the vulnerability to purse seine gears because of a deepening of the thermocline in the main fishing grounds. An inverse response is suggested by Marsac and Le Blanc (in press) on the vulnerability to longline gear. The positive effect of a deepening of the thermocline on yellowfin longline catches can be explained by a greater availability of this tuna at depths where the target species is bigeye in normal climatic conditions.

Discussion

The existence of particular surface conditions promoting the success of recruitment for tunas is not such a surprise, because of an underlying ecological concept, namely the "fundamental triad" (Bakun 1995), already verified in small pelagic fisheries. Like small pelagic fishes, tuna experience a critical larval phase that is controlled by different physical processes. Those described in the triad are enrichment, concentration and retention. Enrichment is the result of upwelling and/or mixing that brings nutrients in the surface layer and consequently boosts the primary and secondary production. Production then needs to be concentrated to be fully available to higher trophic levels (in the present case, larvae feeding upon zooplankton). Finally, the batches of larvae and their preys should not be scattered by strong currents; larvae will benefit from small scale gyring circulation which maintain them in the appropriate habitat, namely the retention area. The turbulence can be seen as a proxy variable of this combination. This parameter is the key parameter of the optimal environmental window proposed by Cury and Roy (1989). With respect to tropical tunas, it is striking to see the good agreement between periods and areas of warm and calm surface conditions and timing and location of the main spawning activity. Too low a turbulence will enhance the spatial integrity of the larvae batches, but enrichment will then be the limiting factor. Conversely, strong turbulence will generate a significant enrichment, but the larvae will be too dispersed to benefit from the biological production bloom.

The direct application of these findings into large pelagic fish communities and the consequences in terms of population dynamics, are not trivial because of the wider geographic scale compared to the small pelagic coastal habitat. There is a great spatial heterogeneity of the oceanographic response to atmospheric forcing. This has to be considered in the analysis, and the EOF decomposition is an efficient tool for this purpose. The sophisticated physiology of large tropical tunas provides them with great flexibility to face environmental anomalies. Apart from the main (and regular) spawning grounds, tropical tunas can also spawn in other areas of the equatorial zone where anomalies might not be as important as in the core spawning zone. Locally, high turbulence seems to be detrimental to larval survival, which can be detected in the age 0 CPUEs in a specific oceanic area. On a larger scale (the ocean basin), it is likely that the variability of recruitment of tropical tunas is not so great. Although a direct link of the recruitment variability can be seen in the adult CPUE, advanced analyses are necessary to verify the relationship at the scale of the stock, using GLMs on different data sets (longline, purse seine, combined…) and VPA.

The trend of the fisheries potential can be approached by an index similar to that proposed by Grainger and Garcia (1996). The index calculated in the present study is very simple, being the ratio between the catch at a year *i* and the average catch of the three previous years (*i-3*). In other terms, it indicates the rate of increase (when more than 1) or of decrease (less than 1) of the catches versus time. Consequently, index values around 1 would suggest that a level of equilibrium is reached (which can correspond to any point on the production curve, before, at or beyond the MSY), under the assumption that the fishing pattern has not changed drastically. The catch data are the figures for all nations and gears in the whole Indian Ocean; that are available in the latest IOTC data Summary (#18). A linear trend was calculated from the series of annual indices (Figure 13). Since the introduction of the industrial purse seine fishery (1983-84), the catches have followed a decreasing trend for yellowfin and skipjack tuna, and the index is now around 1. The environment induces either positive or negative deviation about the trend, with ENSO years explaining some of the negative effects (other unknown factors may also interact to modulate the response). Whereas yellowfin and skipjack trends have very similar slopes, the long-term trend for bigeye is stable. In the early 1990s the

index increased dramatically due to purse seiners fishing more intensively on floating objects with deeper nets. In the case of this species, according to the dominance of longline catches, ENSO years tend to play a positive effect and push the index above the trend in the series prior to 1990.

Conclusion

There is evidence of significant interannual variability of climatic and oceanographic conditions in the Indian Ocean. Most of the anomalies are connected to the Pacific ENSO, but the magnitude of anomalies can be rather independent from those affecting the equatorial Pacific. The development of a warm event in the Indian Ocean is possible because of the relatively large width of the equatorial zone in this ocean compared to the Atlantic where the continental masses play an important role and modulate the ENSO signal. The effect of such interannual variability on the stock and exploitation of yellowfin suggests a stronger effect on catchability than on abundance itself. In the area studied, which encompasses the regular fishing grounds exploited since the beginning of the fishery, the vulnerability to purse seine gears decreases during ENSO events, because of a significant deepening of the thermocline. During the latest (and very strong) ENSO, the collapse of CPUEs in the West pushed the boats to survey the eastern basin where very good catches were recorded in relation to an abnormal rise of the thermocline induced by the ENSO. The reversal of the thermocline slope is explained by the changes in zonal wind stress along the equator. The effect on abundance is mainly driven by the turbulence. Locally, success of recruitment may be affected by a stronger than normal turbulence but the effect at the scale of the stock is not obvious and might not be significant. Direct methods like tagging will help to provide a clearer view of environmental effects on migration patterns and concentration areas.

From the series of the fisheries potential index defined in the previous section, it appears that, after a significant deviation, the index returns about the trend, which suggests that the environmental anomaly is affecting primarily catchability (immediate or short term effects). In some circumstances, the abundance can be affected, but in the present status of stocks (most likely below or at level of full exploitation) a detrimental effect on larval survival in a given location can be compensated by a normal or favorable habitat in another place, according to the large spawning area of the tropical tunas. However, variations of trends in CPUEs or other population indices must be well understood with respect to the environment to be properly integrated in stock assessment analyses particularly if the fishing pressure continues increasing. The response of a stock to environmental anomalies is probably non-linear. Detrimental effects will be more drastic on a heavily exploited resource than on a virgin stock. Consequently, continuous monitoring of the physical environment, from the atmosphere to the ocean, is a task that cannot be avoided in a modern tuna research and should be encouraged in the framework of the future research programme of the Indian Ocean Tuna Commission.

References

Bakun, A. 1995. The California current, Benguela current and southwestern Atlantic shelf ecosystems: a comparative approach to identifying factors regulating biomass yields. *In*: K. Sherman, L.M. Alexander and B. Bold (Eds*). Large marine ecosystems: stress, mitigation and sustainability*. Am. Assoc. For the Advancement of Science: 199-224.

Barnett, T.P. 1983. Interaction of the monsoon and Pacific trade wind system at interannual time scales. Part I: the equatorial zone. *Monthly Weather Rev*., 111: 756-773.

Barnett, T.P. 1984a. Interaction of the monsoon and Pacific trade wind system at interannual time scales. Part II: the tropical band. *Monthly Weather Rev*., 112: 2380-2387.

Barnett, T.P. 1984b. Interaction of the monsoon and Pacific trade wind system at interannual time scales. Part III: a partial anatomy of the Southern Oscillation. *Monthly Weather Rev*., 112: 2388-2400.

Barnett, T.P. 1991. The interaction of multiple time scales in the tropical climate system. *Journal of Clim*., 4: 269-285.

Breiman, L. and J.H. Friedman. 1985. Estimating optimal transformations for multiple regression and correlation. *J. Am. Stat. Assoc*., 80: 580-619.

Cury, P. and C. Roy. 1989. Optimal environmental window and pelagic fish recruitment success in upwelling areas. *Can. J. Fish. Aquat. Sci*., 46:670-680.

Gascuel, D., A. Fonteneau et E. Foucher. 1993. Analyse de l'évolution des puissances de pêche par l'analyse des cohortes: application aux senneurs exploitant l'albacore (*Thunnus albacares*) dans l'Atlantique Est*. Aquat. Living resour*., 6: 15-30

Grainger, R.J.R. and S. Garcia. 1996. Chronicles of marine fishery landings (1950-1994). Trend analysis and fisheries potential. *FAO Fish. Tech. Pap*., 359, 51 p.

Lasker, R. (Ed). 1981. Marine fish larvae. Morphology, ecology and relation to fisheries. University of Washington Press, Seattle and London.

Levitus, S. and T.P. Boyer. 1994. World Ocean Atlas 1994. US Dept Comm., NOAA, NESDIS.

Lorenz, E. 1956. Empirical orthogonal functions and statistical weather predictions. Rep. N° 1, Statistical Forecasting Programme, MIT: 49 p.

Marsac, F. 1992. Etude des relations entre l'hydroclimat et la pêche thonière hauturière tropicale dans l'océan Indien occidental. Thèse de Doctorat, Université de Bretagne Occidentale, 353 p.

Marsac, F. 1998a. L'environnement océanique et son impact sur la pêche thonière hauturière: des relations individuelles aux processus générés à l'échelle de l'océan. *In*: P. Cayré et J-Y. Le Gall (Eds*). Le thon: enjeux et stratégies pour l'océan Indien. Tuna prospects and strategies for the Indian Ocean.* Actes de la Conférence thonière internationale 1996. Proceedings of the International Tuna Conference 1996, 27, 28, 29 nov. 1996, Maurice. COI/ORSTOM, Paris, collection *Colloques et Séminaires*: 139-176.

Marsac, F. 1998b. Changements hydroclimatiques observés dans l'Atlantique depuis les années 50 et impacts possibles sur quelques stocks de thons et leur exploitation. *Working Document ICCAT*, SCRS/98/135, 27 p.

Marsac, F. and J.L. Le Blanc (in press). Interannual and ENSO-associated variability of the coupled ocean-atmosphere system with possible impacts on the yellowfin tuna fisheries of the Indian and Atlantic oceans. Symposium ICCAT, Ponta Delgada, Acores, June 1996.

Meehl, G.A. 1987. The annual cycle and interannual variability in the tropical Pacific and Indian Ocean regions. *Monthly Weather Rev*., 115: 27-50.

Menselssohn, R. and C. Roy. 1996. Comprehensive Ocean data Extraction users guide*. US Dept. Comm., NOAA Tech.*

Memo. NOAA-TM-NMFS-SWFSC-228, La Jolla, CA: 67 p.

Parrish, R.H., C.S. Nelson and A. Bakun. 1981. Transport mechanisms and reproductive success of fishes in the California Current. *Biol. Oceanogr* 1(2).

Peterman, M.R., and M.J. Bradford. 1987. Wind speed and mortality rate of a marine fish, the northern anchovy *(Engraulis mordax). Science*, 235: 354-356.

Slutz, R.J., S.J. Lubker, J.D. Hiscox, S.D. Woodruff, R.L. Jenne, D.H. Joseph, P.M. Steurer and J.D. Elms. 1985. Comprehensive Ocean Atmosphere Data Set; release 1. NOAA Environmental Research Laboratories, Climate Research Program, Boulder, CO, 268 p.

Suzuki, Z. 1988. Study of interaction between longline and purse seine fisheries on yellowfin tuna *Thunnus albacares* (Bonnaterre). *Bull. Far Seas Fish. Lab.,* 25: 73-144.

Tomczak, M. and J.S. Godfrey. 1994. Regional Oceanography: an introduction. Pergamon Press.

Woodruff, S.D., R.J. Slutz, R.L. Jenne and P.M. Steurer. 1987. A comprehensive Ocean-Atmosphere Data Set. *Bull. Amer. Meteor. Soc*., 68: 1239-1250.

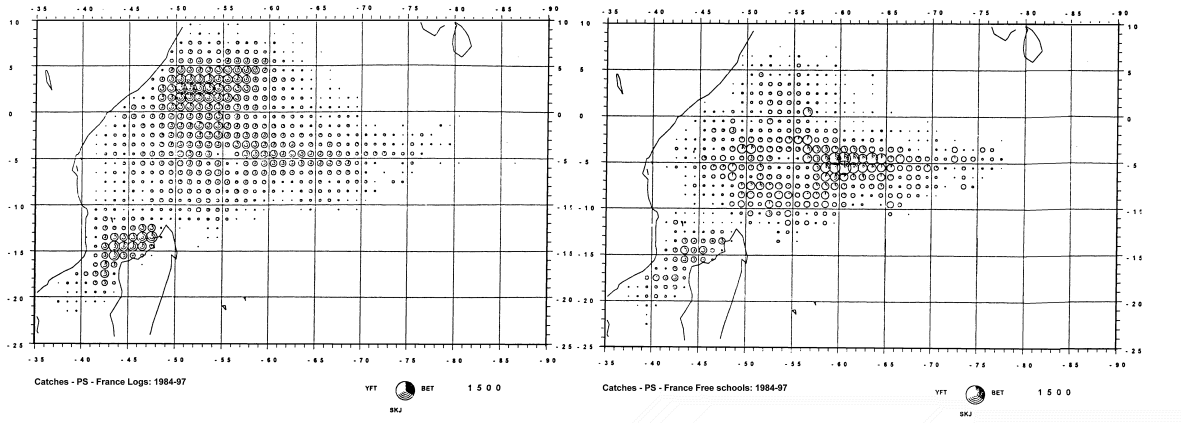

Figure 1: French purse seine catches on floating objects (left) and on free-swimming schools (right). Skipjack is the main target species on logs and yellowfin is dominant in free schools (average catches 1984-97).

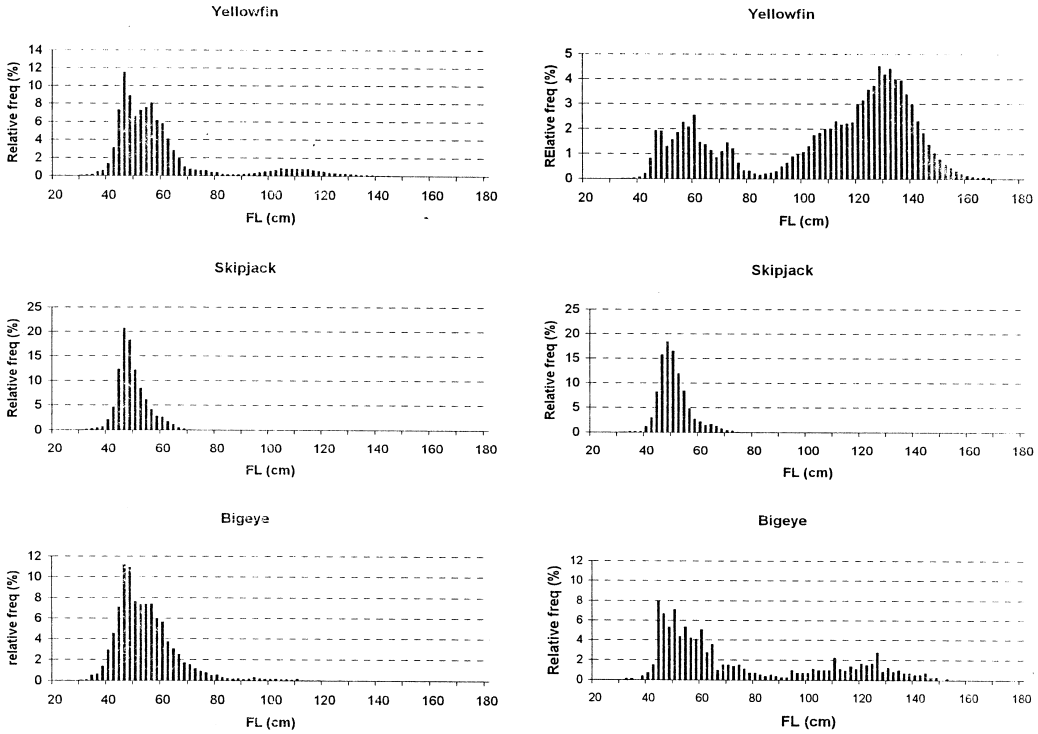

Figure 2: Size distribution (in numbers) of French purse seine catches on floating objects (a) and on free-swimming schools (b).

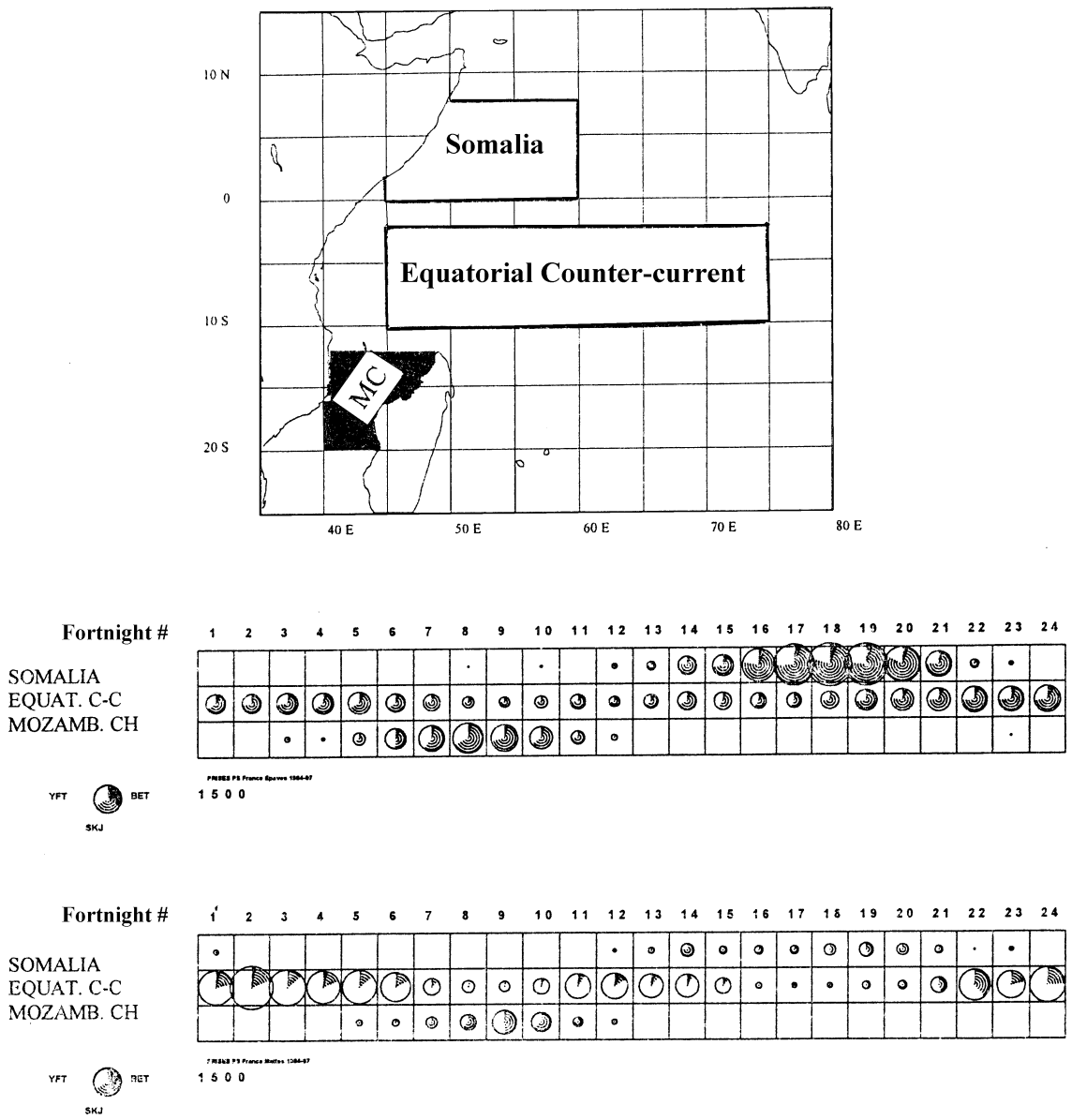

Figure 3: Distribution of French purse seine catches: breakdown by species, area and fortnight for floating objects (top) and free-swimming schools (bottom) – average 1984-97

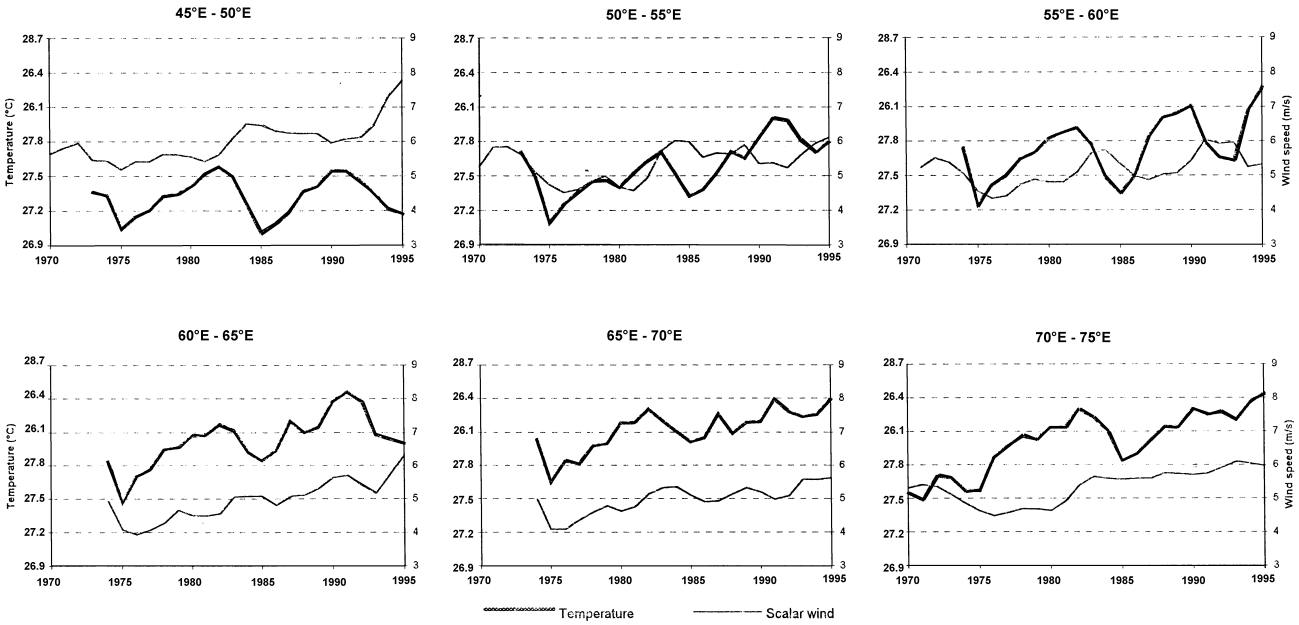

Figure 4: Trends of SST and scalar wind by 5° longitude boxes in the ECC area (2°S-10°S)

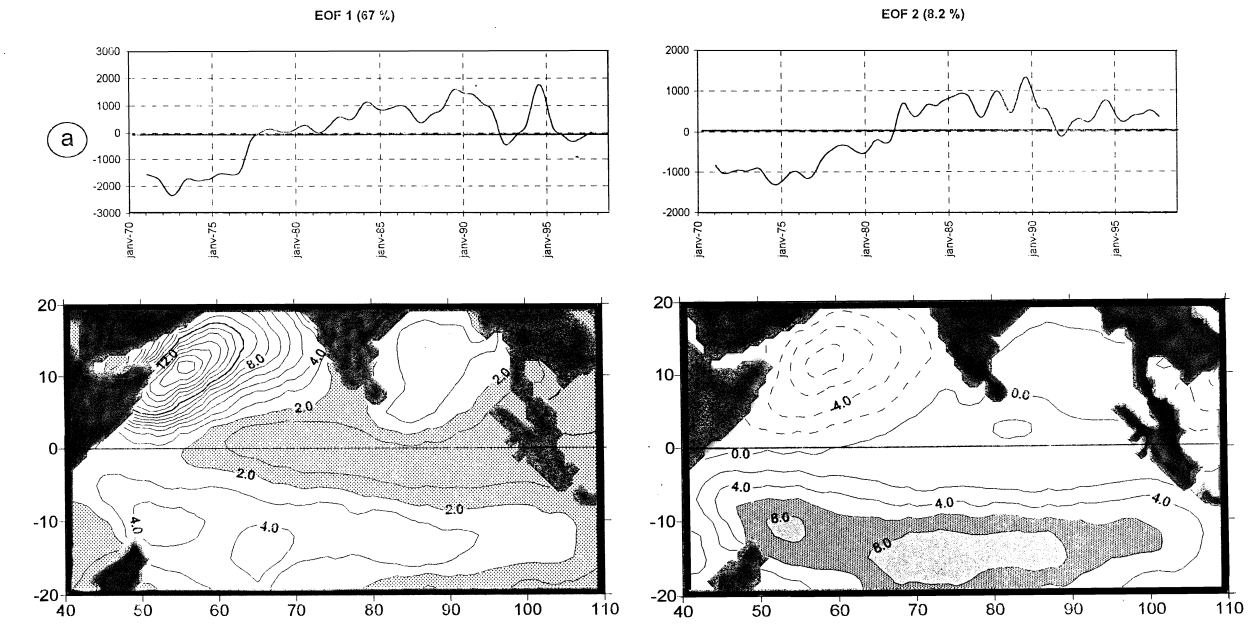

Figure 5: EOF analysis of the turbulence (wind speed cubed) in the Indian Ocean. Time series of the EOF coefficients (a) and spatial pattern of the variability (b). The time series is filtered on 12 months using a low pass cosine filter.
(The turbulence is strongest in the Somali Basin and weakest in the Mozambique Channel. The time series indicate that the turbulence has increased from the mid-70s and that two collapses were recorded in 1992 and 1996)

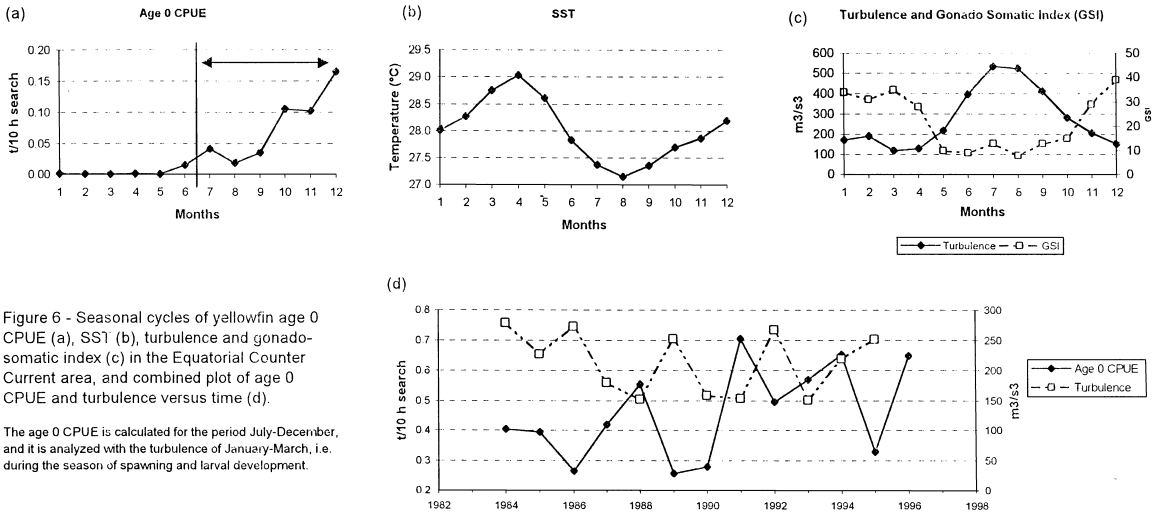

Figure 6 - Seasonal cycles of yellowfin age 0 CPUE (a), SST (b), turbulence and gonado-somatic index (c) in the Equatorial Counter Current area, and combined plot of age 0 CPUE and turbulence versus time (d).

The age 0 CPUE is calculated for the period July-December, and it is analyzed with the turbulence of January-March, i.e. during the season of spawning and larval development.

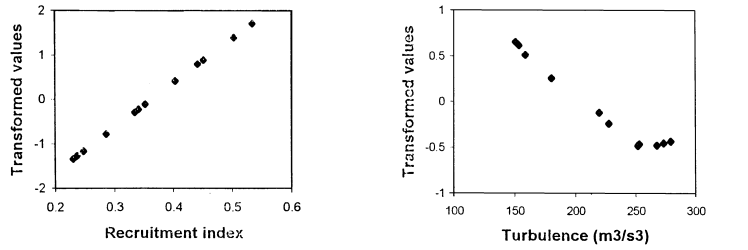

Figure 7 - Optimal empirical transformations from the ACE algorithm on yellowfin age 0 CPUE (July-December) and turbulence (January-March). 12 years series (1984-95). R^2 = 25.8 %

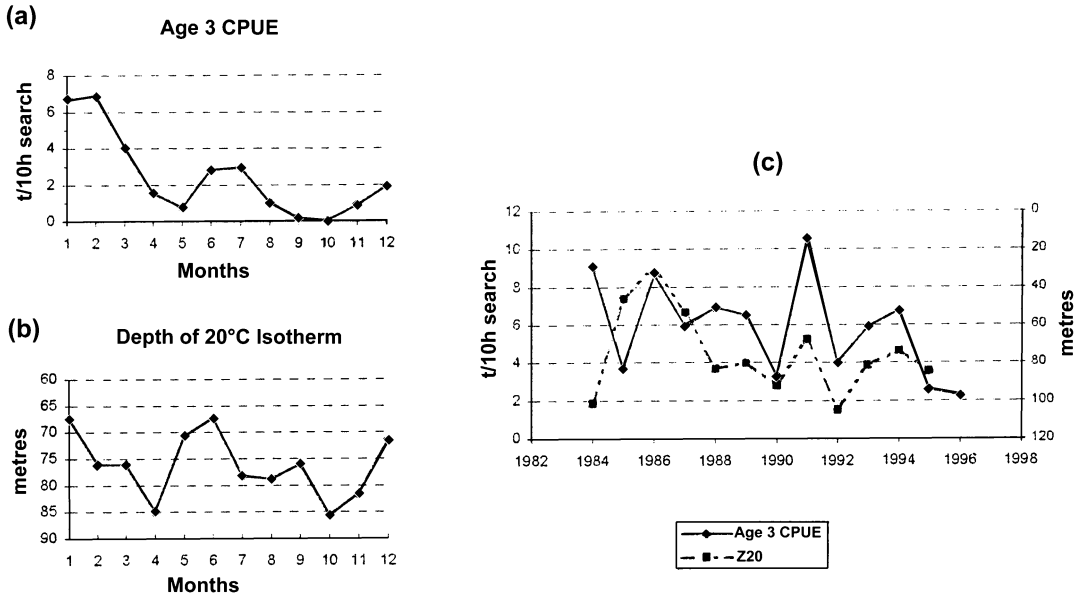

Figure 8: Seasonal cycle of yellowfin age 3 CPUE (a), depth of 20°C isotherm (b) and combined plot of both parameters versus time (c) (The age 3 CPUE and depth of 20°C isotherm are calculated during January-March)

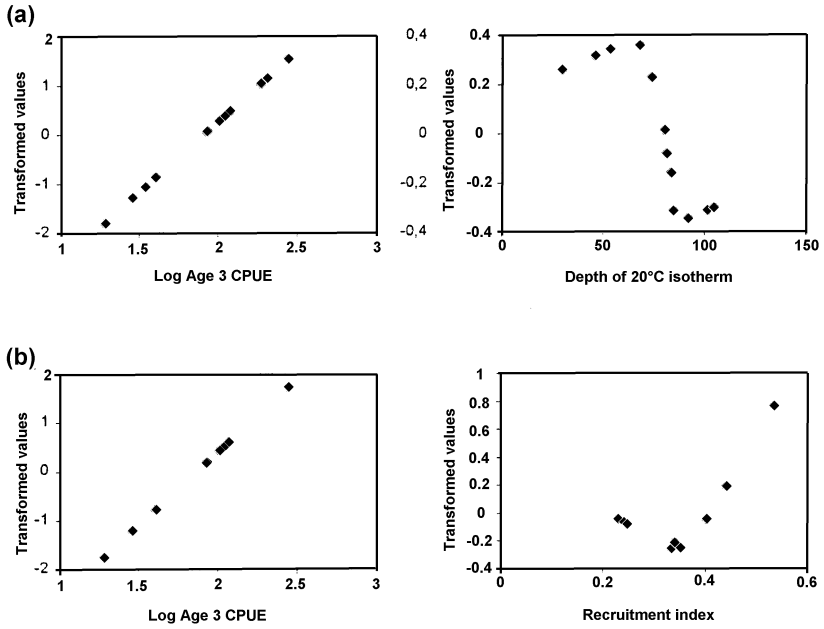

Figure 9: Optimal empirical transformations from the ACE algorithm.
(a) dependent variable Log age 3 CPUE during January-March (1984-95); independent variable isotherm 20°C depth during same period; R^2=16.4 %
(b) dependent variable Log age 3 CPUE during January-March (1984-95); independent variable recruitment index lagged 3 years before (1984-92); R^2= 11.4 %)

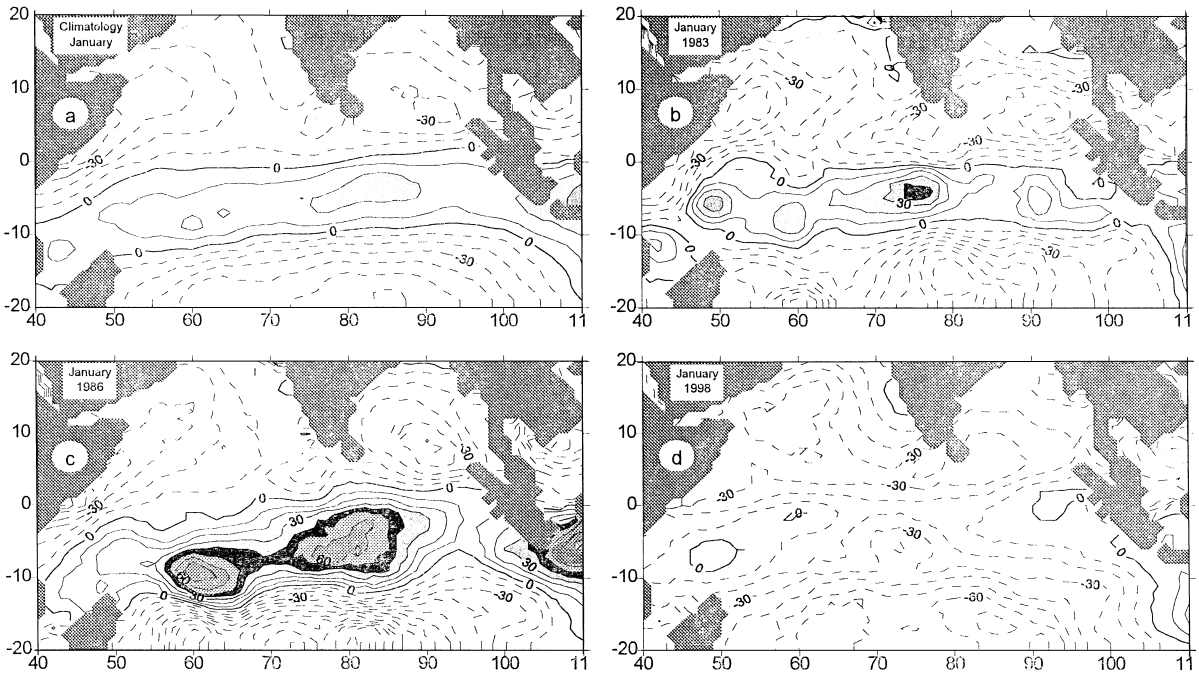

Figure 10: Zonal wind stress field in January from the Florida State University data set. The ENSO conditions are represented in (b) and (d), and the opposite situation (La Niña type) in (c).

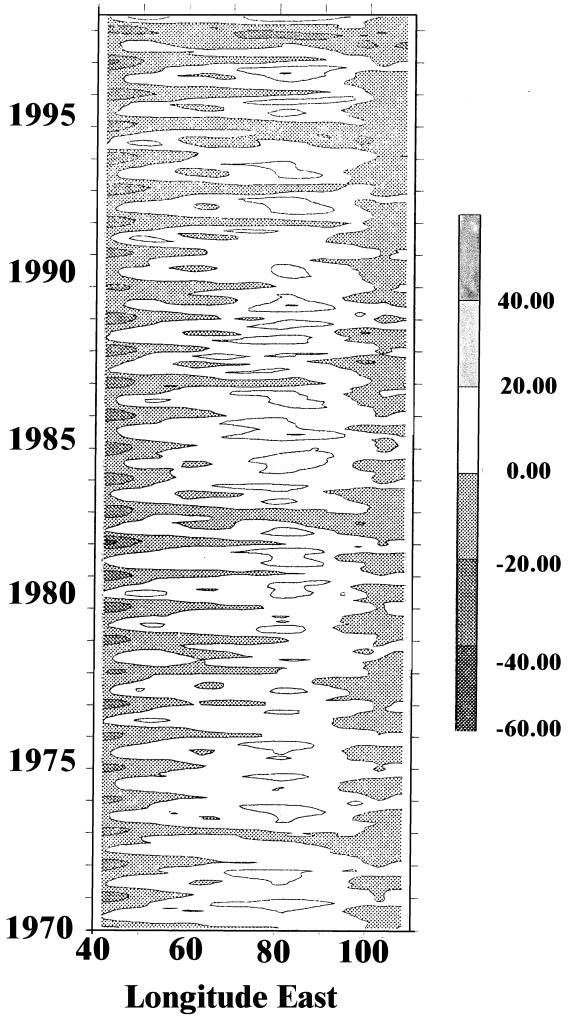

Figure 11 - Monthly values of zonal wind stress in the equatorial area 5°N-5°S, plotted versus the longitude, from January 1970 to July 1998. The negative values (medium and dark grey) denote easterlies, whilst light grey area denote westerlies. The ENSO conditions are characterized by easterlies in December-January generating shallow thermocline in the East and deep thermocline in the West.

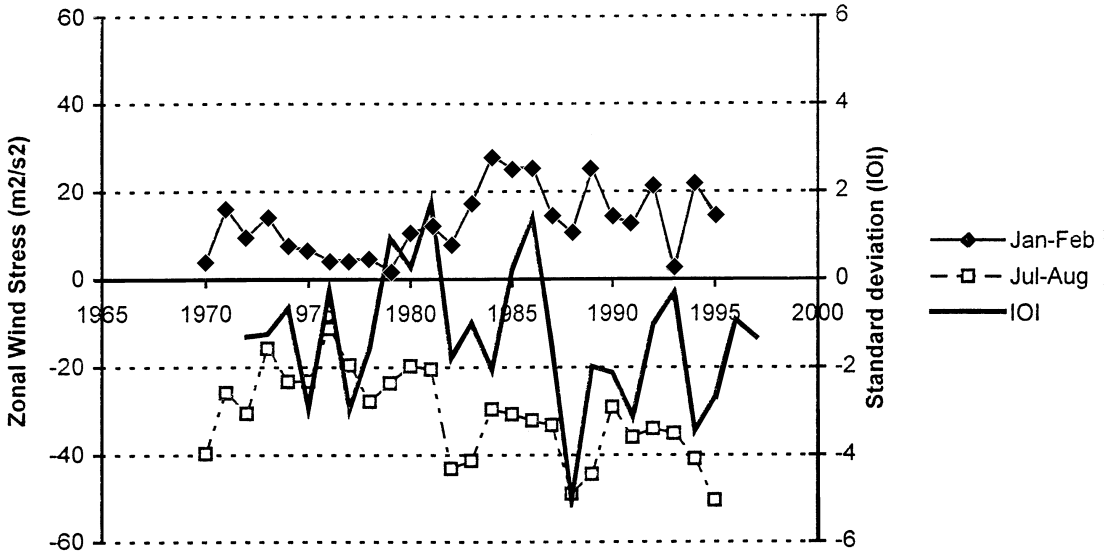

Figure 12- Combined plot of zonal wind stress in January-February and in July-August, and the Indian Ocean Index (annual average), in the Equatorial Counter Current area (2°-10°S). The correlation between IOI and January-February is not significant at 5 % probability risk whist it is highly significant (r = 0.48) with the July-August wind stress. This denotes a strengthening of trade winds in the Indian Ocean during El Niño.

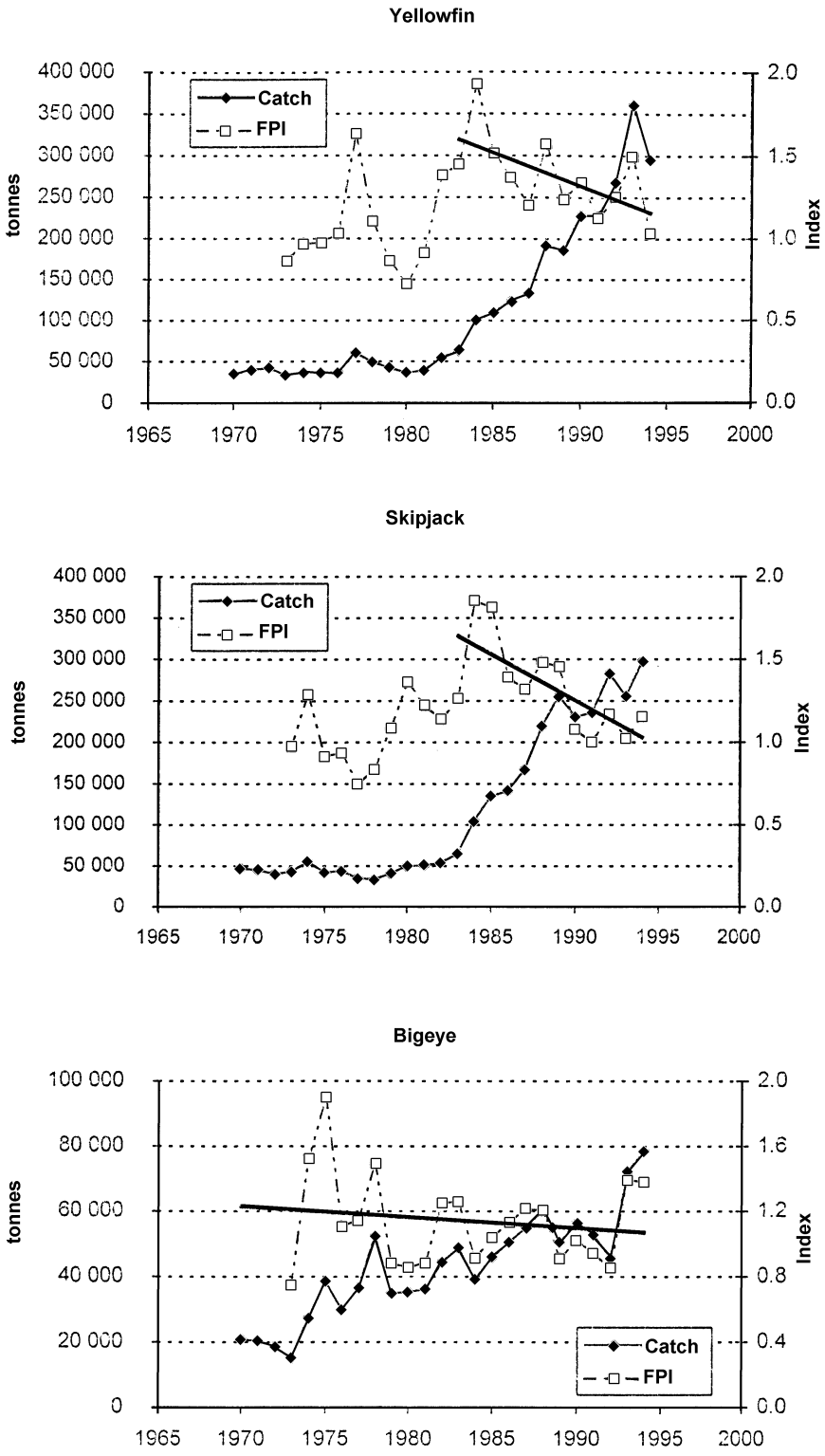

Figure 13- Trend of the total catches by species in the Indian Ocean (FAO areas 51 and 57) and "fisheries potential index" (FPI). This index is the relative increase of catch between a year i and the mean of the catches recorded between the three previous years (i-1, i-2, i -3). This index denotes the increasing (if greater than 1) or decreasing (less than 1) rate of the catches. For the three species considered, the latest values are still sligtly above 1, but a significant decreasing trend has been recorded for yellowfin and skipjack.